J|A|C|S
ARTICLES
Published on Web 03/22/2006

Probing Lipid Vesicles by Bimolecular Association and Dissociation Trajectories of Single Molecules

Feng Gao, Erwen Mei, Manho Lim,† and Robin M. Hochstrasser*
Contribution from the Department of Chemistry, University of Pennsylvania, Philadelphia, Pennsylvania 19104
Received December 9, 2005; E-mail: hochstra@sas.upenn.edu

Abstract: Vesicles prepared by DMPC (1,2-dimyristoyl-*sn*-glycero-3-phosphocholine) and SOPC (1-stearoyl-2-oleoyl-*sn*-glycero-3-phosphocholine) lipid molecules having sizes smaller than the diffraction-limited focused laser beam have been used to confine single molecules in the laser focus. The confinement of single molecules in a volume smaller than the focused laser beam leads to a Gaussian distribution of single molecule fluorescence intensity. The interactions of single Nile Red molecules with DMPC and SOPC lipid bilayers were studied by single molecule fluorescence confocal microscopy. Nile Red molecules were observed to associate with and dissociate from individual DMPC and SOPC vesicles adsorbed on a glass surface, generating on-and-off fluctuations in a fluorescence signal representing a very low noise two-state trajectory. Off-time statistics were used to investigate the mean radius of the vesicles and the size distribution functions. The means of the on-time distributions of Nile Red in DMPC and SOPC vesicles were significantly different. The association and dissociation reactions of single Nile Red molecules with a vesicle have been studied. Features of the bimolecular interaction between the probe Nile Red and the vesicle were evaluated from the uncorrelated mean on-time and vesicle radius distributions, and the linear Nile Red concentration dependence of the mean off-time. Nile Red is shown to be a useful probe of the structural fluctuations and heterogeneity of these membrane structures, and it is a useful model with which to directly study a diffusion-influenced reversible bimolecular reaction.

Introduction

Biological membranes are dynamic, heterogeneous structures that have many functional units or organelles that are highly specialized and contain proteins and lipid components that perform unique roles for that organelle. Membrane components have roles that range from regulation, binding of signaling molecules, protection, recognition, provision of anchoring and stable sites for binding and catalysis, compartmentalization of domains, regulation of the fusion of membranes in the cell, and provision of routes across the membrane to allow directed cell or organelle motility. These cellular processes are expected to be strongly coupled to the physical properties of membranes, including fluidity, microdomain formation, chemical content, and dynamics. Therefore, fundamental knowledge of membrane physical processes, heterogeneity (e.g., lipid rafts),[1−3] structural dynamics, and structural variability at a molecular level is needed to help understand cell physiology. Supported lipid bilayers created by vesicle fusion have been used to model cell−cell interactions.[4] They have been shown to be useful mimics for natural biological membranes. Large, unilamellar phospholipid vesicles (LUVs) can also serve as models for biological membranes. These LUVs stick to glass surfaces,[5] as do live cells, and at sufficiently low concentrations of vesicles, they remain spatially separated from one another. This feature facilitates their examination on a vesicle-by-vesicle basis[5] by means of fluorescence techniques.

Single molecule fluorescence correlation spectroscopy (FCS) has proved to be a very powerful technique, in which individual molecules are detected when they diffuse through a small probe volume defined by a focused laser beam and confocal optics.[6,7] In FCS, the residence time for a molecule staying in a fixed probe volume is determined by the diffusion coefficient of the molecule in the medium, which is usually less than 1 ms. Some slow dynamical processes, such as conformational changes of proteins, escape detection in such a brief sojourn within the laser field. It is therefore valuable to develop approaches that confine individual molecules to the probe volume[8,9] and simultaneously provide a well-defined environment[10] for the target molecules. In the present work we describe a method in which a particle that is much smaller than the size of the focused laser beam is used to confine the target molecules to the probe volume. The confining particle is a vesicle. The fluorescence

† Current address: Department of Chemistry, Pusan National University, Busan, Korea.

(1) Edidin, M. *Curr. Opin. Struct. Biol.* **1997**, *7*, 528−532.
(2) Dietrich, C.; Bagatolli, L. A.; Volovyk, Z. N.; Thompson, N. L.; Levi, M.; Jacobson, K.; Gratton, E. *Biophys. J.* **2001**, *80*, 1417−1428.
(3) Maxfield, F. R. *Curr. Opin. Cell. Biol.* **2002**, *14*, 483−487.
(4) Brain, A. A.; McConnell, H. M. *Proc. Natl. Acad. Sci. U.S.A.* **1984**, *81*, 6159−6163.
(5) Johnson, J. M.; Ha, T.; Chu, S.; Boxer, S. G. *Biophys. J.* **2002**, *83*, 3371−3379.
(6) Elson, E. L.; Webb, W. W. *Annual Review of Biophysics and Bioengineering Field* **1975**, *4*, 311−334.
(7) Eigen, M.; Rigler, R. *Proc. Natl. Acad. Sci. U.S.A.* **1994**, *91*, 5740−5747.
(8) Mei, E.; Sharonov, A.; Gao, F.; Ferris, J. H.; Hochstrasser, R. M. *J. Phys. Chem. A.* **2004**, *108*, 7339−7346.
(9) Chiu, D. T.; Zare, R. N. *J. Am. Chem. Soc.* **1996**, *118*, 6512−6513.
(10) Van Horn, W. D.; Simorellis, A. K.; Flynn, P. F. *J. Am. Chem. Soc.* **2005**, *127*, 13553−13560.

10.1021/ja058098a CCC: $33.50

of a Nile Red probe is only detected when it collides with the vesicle. In the experiments, single Nile Red molecules are repeatedly detected through observations of their fluorescence from a confocal region of the microscope, which brackets only one immobilized vesicle. The fluctuations in the Nile Red fluorescence relate to the size, heterogeneity, and fluctuations of vesicles located in the focused laser beam. Since single molecules are used as probes, the lipid bilayers are not expected to be perturbed significantly during the measurement, so that the membrane thermodynamic and kinetic properties, such as structural fluctuations and phase segregation, would be minimally influenced. Furthermore, the relatively small size of the Nile Red probe permits the nanometer scale spatial dimension of the lipid bilayer to be estimated from the statistics of the collisions.

Nile Red is a sensitive probe for polarity and hydrophobicity.[11−13] It emits negligible fluorescence in the presence of bulk water. It has absorption, fluorescence, fluorescence lifetimes, and fluorescence quantum yields that depend on the solvent polarity. The spectral sensitivity of Nile red to solvent polarity is attributed to a twisted internal charge-transfer (TICT) configuration involving motions of the diethylamino group.[14,15] Single Nile Red molecules in aqueous solution are not readily detectable by fluorescence methods since the fluorescence of Nile Red is quenched by water. However, it has been shown that Nile Red emits significant fluorescence when bound to hydrophobic materials, such as phospholipid membranes,[16] and fluorescence signals from single Nile Red molecules are detectable when Nile Red is in the hydrophobic environments[13,17] or Nile Red bound to the hydrophobic pocket of a protein.[12]

The method described here can also be regarded as an approach with which to study diffusion-influenced reversible bimolecular reactions. By monitoring the rate of fluorescence bursts, and the duration of fluorescence signals, the association and dissociation reaction rates can be measured. This situation is analogous to reactions between enzymes and their cofactors which have been reported at the single molecule level and show on- and off-state trajectories,[18−20] and it is also analogous to studies of "blinking" of nanoparticles.[21] The theory of the origins and analysis of single molecule on and off trajectories is well established.[22−25] With the knowledge of the concentration of Nile Red in solution, the equilibrium constant can be calculated.

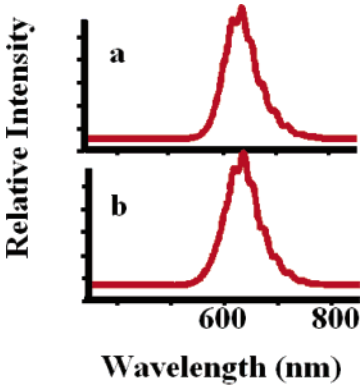

Figure 1. Bulk fluorescence spectra of Nile Red bound to DMPC (peak 628 nm) and SOPC (peak 630 nm) lipid bilayers on a glass surface. The spectra are recorded on a confocal microscope equipped with a monochromator and CCD camera.

The theory of the kinetics of irreversible[26] and reversible bimolecular reactions[27−29] has been widely studied. There are features that are difficult to confirm in bulk experiments: for example, the power law relaxation of the concentrations near equilibrium. The theory has been tested in bulk experiments[30] where very small changes in the concentration from equilibrium on long time scales were examined that are difficult to monitor. The types of single molecule experiments described here may eventually provide easier access to such subtleties in the kinetics of reversible bimolecular reactions.

Materials and Methods

Materials. Nile Red was purchased from Molecular Probes and used as received. Glass coverslips and cylinders were purchased from Fisher. These were cleaned by sequential sonication in 2 M sodium hydroxide solution, methanol, 2 M sodium hydroxide solution, and deionized water. 1,2-Dimyristoyl-*sn*-glycero-3-phosphocholine (DMPC) and 1-stearoyl-2-oleoyl-*sn*-glycero-3-phosphocholine (SOPC) were purchased from Avanti Polar Lipids. DMPC and SOPC have the same headgroups. Both C_{14} hydrocarbon chains in DMPC are saturated, but one of the C_{18} chains in SOPC has a double bond. The phase transition temperature of DMPC is ∼24 °C, and that of SOPC is 6 °C. These lipids carry zero net charge at pH 7.4. The fluorescence spectra of bulk Nile Red molecules bound to DMPC and SOPC lipid bilayers on a glass surface are shown in Figure 1a and 1b, respectively.

Vesicle Preparation. To prepare large unilamellar vesicles, we used the following procedure:[5,31] 0.25 mL of 25 mg/mL DMPC or SOPC lipids was contained in a vial, and a nitrogen flow was used to evaporate the solvent chloroform, leaving a dry phospholipid film on the internal surface of the vial. The vial was kept under vacuum for 2 h before the lipid film was allowed to hydrate in 4 mL of phosphate buffer (20 mM, pH 7.0) with vigorous stirring at 32 °C for 1.5 h. The resulting multilamellar vesicles were subjected to five freeze/thaw cycles and extruded about 20 times through polycarbonate membranes having a 100 nm pore diameter (Avanti Mini-Extruder). Vesicles were used within 1 or 2 days of preparation. The concentration of the vesicles used in the single molecule experiment is ∼1 pM to make sure that individual vesicles adsorbed on the glass surface are well isolated from one another.

(11) Sackett, D. L.; Knutson, J. R.; Wolff, J. *J. Biol. Chem.* **1990**, *265*, 14899−14906.
(12) Tang, J.; Mei, E.; Green, C.; Kaplan, J.; DeGrado, W. F.; Smith, A. B., III; Hochstrasser, R. M. *J. Phys. Chem. B* **2004**, *108*, 15910−15918.
(13) Hou, Y.; Bardo, A. M.; Martinez, C.; Higgins, D. A. *J. Phys. Chem. B* **2000**, *104*, 212−219.
(14) Cser, A.; Nagy, K.; Biczok, L. *Chem. Phys. Lett.* **2002**, *360*, 473−478.
(15) Dutta, A. K.; Kamada, K.; Ohta, K. *J. Photochem. Photobiol., A* **1996**, *93*, 57−64.
(16) Krishnamoorthy, I. G. *Biochim. Biophys. Acta* **1998**, *1414*, 255−259.
(17) Martin-Brown, S. A.; Fu, Y.; Saroja, G.; Collinson, M. M.; Higgins, D. A. *Anal. Chem.* **2005**, *77*, 486-494.
(18) Zhang, Z.; Rajagopalan, P. T. R.; Selzer, T.; Benkovic, S. J.; Hammes, G. G. *Proc. Nat. Acad. Sci. U.S.A.* **2004**, *101*, 2764−2769.
(19) Lu, H. P.; Xun, L.; Xie, S. X. *Science* **1998**, *282*, 1877−1882.
(20) Flomenbom, O.; Velonia, K.; Loos, D.; Masuo, S.; Cotlet, M.; Engelborghs, Y.; Hofkens, J.; Rowan, A. E.; Nolte, R. J. M.; Van der Auweraer, M.; De Schryver, F. C.; Klafter, J. *Proc. Nat. Acad. Sci. U.S.A.* **2005**, *102*, 2368−2372.
(21) Nirmal, M.; Dabbousi, B. O.; Bawendi, M. G.; Macklin, J. J.; Trautman, J. K.; Harris, T. D.; Brus, L. E. *Nature* **1996**, *383*, 802−804.
(22) Margolin, G.; Barkai, E. *J. Chem. Phys.* **2004**, *121*, 1566−1577.
(23) Verberk, R.; Orrit, M. *J. Chem. Phys.* **2003**, *119*, 2214−2222.
(24) Flomenbom, O.; Klafter, J. *J. Chem. Phys.* **2005**, *123*, 64903−64910.
(25) Flomenbom, O.; Klafter, J.; Szabo, A. *Biophys. J.* **2005**, *88*, 3780−3783.
(26) Smoluchowski, M. V. *Phys. Z.* **1916**, *17*, 557.
(27) Agmon, N.; Szabo, A. *J. Chem. Phys.* **1990**, *92*, 5270−5284.
(28) Gopich, I. V.; Ovchinnikov, A. A.; Szabo, A. *Phys. Rev. Lett.* **2001**, *86*, 922−925.
(29) Lee, S.; Karplus, M. *J. Chem. Phys.* **1986**, *86*, 1883−1903.
(30) Huppert, D.; Goldberg, S. Y.; Masad, A.; Agmon, N. *Phys. Rev. Lett.* **1992**, *68*, 3932−3935.
(31) Boukobza, E.; Sonnenfeld, A.; Haran, G. *J. Phys. Chem. B* **2001**, *105*, 12165−12170.

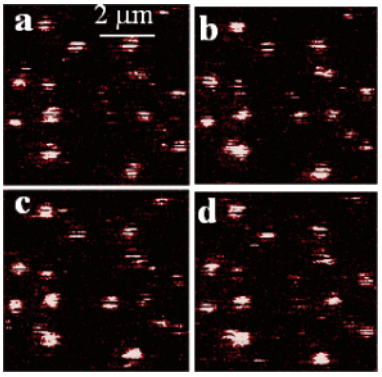

Figure 2. Four fluorescence images of a glass surface covered by 100 μL of 40 mM pH 7.0 buffer solution containing ~1 pM DMPC vesicles and ~0.4 nM Nile Red. The size of each image is 6.83 μm × 6.83 μm. The images were obtained sequentially with 26 s being required for each image.

Microscopy. The scanning confocal microscope, described previously,[32] uses a sample-scanning stage (Queensgate) with closed-loop X−Y feedback for accurate sample positioning and location of individual molecules. The stage is controlled by a modified Nanoscope E controller (Digital Instruments). The sample and stage were mounted on an inverted, epiilllumination microscope (Nikon, Diaphot 300). The 514.4 nm line from an Ar ion laser or a 76 MHz mode-locked Nd:YAG laser (Coherent Antares) frequency doubled to 532 nm, circularly polarized, was employed to excite the sample. The excitation power was maintained between 30 and 35 μW. A Nikon FLUOR 40×, 1.3 numerical aperture (NA) objective was used to produce a nearly diffraction limited focus on the sample and to collect the fluorescence. 514-nm notch (Kaiser Optical), D605/55 band-pass, 527DCLP dichroic filter, and other appropriate filters were used to spectrally isolate the signals from the excitation laser and background signal. A pinhole with the diameter of 150 μm was also used to suppress the background signal. A single-photon-counting avalanche photodiode was used to detect single fluorescent photons. The fluorescence spectra were obtained by means of a monochromator (Acton Research) equipped with a back-illumination liquid nitrogen cooled CCD camera (Princeton Instruments, Trenton, NJ).

Results

Individual nonfluorescent DMPC vesicles adsorbed on a glass surface were detected by the probe Nile Red, as shown in Figure 2. Figure 2 shows four sequential scanning fluorescence images of a glass plate covered by 100 μL of 40 mM pH 7.0 buffer solution containing ~1 pM DMPC vesicles and ~0.4 nM Nile Red. The fluorescence spots in Figure 2 prove to be the results of the interactions between Nile Red molecules and DMPC vesicles immobilized on glass: the spectra of the fluorescent spots are consistent with those of Nile Red molecules bound to DMPC vesicles in bulk. The same glass surface in the presence of either a similar Nile Red solution or a DMPC vesicle solution is found to have no significant fluorescence. Nile Red emits negligible fluorescence in the buffer solution, so the adsorbed vesicles must present an environment that is able to enhance the Nile Red emission. As can be seen from Figure 2, the observed fluorescence spots are not moving significantly on the length scale of the microscope resolution, which suggests that the vesicles adhere to the surface on time scales much longer than a scan. The average diameter of the vesicles used in the experiments is ~100 nm, which is much smaller than the $1/e^2$ width of the focused laser beam, 500−600 nm, so most of the fluorescence spots in Figure 2 appear as if they were single molecules. These single-molecule-like fluorescence spots are switching on and off but are not photobleaching. By zooming into the area where a fluorescence spot is located, a fluorescence intensity−time record is obtained that is composed of sequential bursts of fluorescence photons separated by relatively longer dark periods when there is no emission, as shown in Figures 3 and 4. The widths of the fluorescence bursts in the intensity−time record clearly correspond to the residence times of single fluorescent Nile Red molecules on the vesicle. The dark periods correspond to the waiting times between successive binding events during which the Nile Red molecules are in water and have undetectable fluorescence. The single-step character of the fluorescence signal for most fluorescence bursts shown in Figures 3 and 4a_1 suggests that each burst corresponds to a single Nile Red molecule interacting with the vesicle.

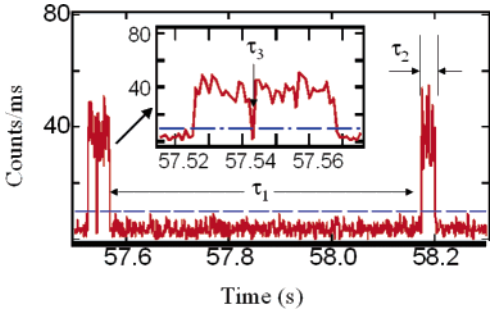

Figure 3. An expanded view of the fluorescence bursts obtained at very low Nile Red concentration in solution (~0.05 nM). The dashed lines show the threshold used to separate background signals from fluorescence bursts. The inset is an expanded view of the first fluorescence burst. A typical diffusion controlled off-time is τ_1, a typical on-time is τ_2, and a typical fast off-time is indicated by τ_3.

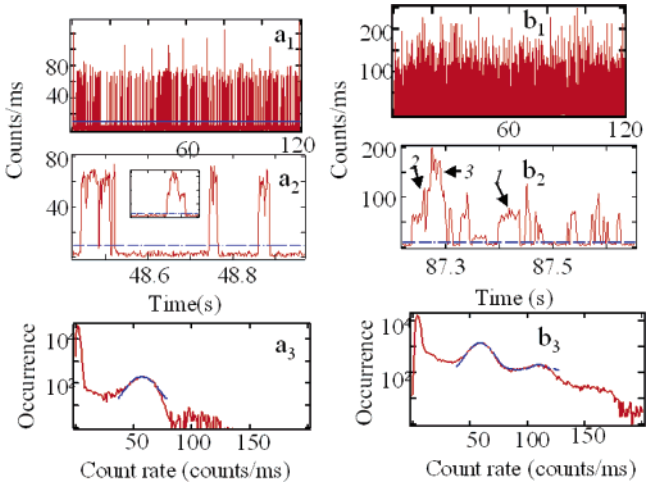

Figure 4. Typical fluorescence intensity−time records (a_1 and b_1) collected with different Nile Red concentrations showing single Nile Red molecules diffusing onto and dissociating from a DMPC vesicle adsorbed on a glass surface and the corresponding expanded views (a_2 and b_2) of a_1 and b_1. The concentrations used are ~0.1 nM (a) and ~1.5 nM(b), respectively. The inset in a_2 shows a fluorescence burst of two Nile Red molecules interacting with one vesicle. The dashed horizontal lines in a_2 and b_2 show the threshold. The labels of 1, 2, and 3 in b_2 indicate fluorescence intensity spikes corresponding to one, two, and three molecules on one vesicle. The corresponding count rate distributions (a_3 and b_3) are calculated based on the intensity−time records in a_1 and b_1. The dashed curves in a_3 and b_3 are Gaussian fits. The means and widths of the Gaussian fits are 57 counts/ms, 11.3 (a_3) and 57 counts/ms, 11.3 and 110 counts/ms, 11.4 (b_3), respectively.

(32) Bopp, M. A.; Sytnik, A.; Howard, T. D.; Cogdell, R. J.; Hochstrasser, R. M. *Proc. Natl. Acad. Sci. U.S.A.* **1999**, *96*, 11271−11276.

The intensity−time records in Figures 3 and 4 are analogous to those collected in FCS, where fluorescence bursts are detected as individual single molecules diffuse through the confocal volume defined by a laser beam focused by confocal optics. The distribution of intensities of the individual bursts shown in Figure 4a_3 clearly indicates the uniqueness of the intensity−time records collected in the present experiments. The count rate distribution consists mainly of two Gaussian peaks. The strong peak centered at 2 counts/ms stems from the background signals, indicating that, during most of the time, no fluorescence signal was detected. The second peak centered at ∼57 counts/ms arises from the detected fluorescence bursts. In FCS, the count rate distribution usually exhibits a super-Poissonian behavior due to the Poisson characteristics of the background signals and the laser intensity profile in the confocal volume.[7,33] The Gaussian distribution of fluorescence signals in the present experiment strongly suggests that the detected individual molecules are confined in a relatively small volume, where both the excitation laser intensity and environment are approximately uniform. A typical vesicle is ∼100 nm in diameter, which is much smaller than the diffraction-limited size of the laser beam. When such a vesicle is located in the middle of the focused laser beam, the light intensity at each point in the vesicle should not vary by more than ca. 6%. The nearly uniform excitation power at the vesicle and a nearly homogeneous environment of the bound probes would lead to a Gaussian profile for the count rate distribution, as observed.

Figure 4a_1 shows there are a few (ca. 10 in this Figure) fluorescence bursts with a significantly higher count rate than the average. Those high intensity fluorescence bursts generally show a steplike character, as shown in the inset of Figure 4a_2, and their peak intensity is roughly twice the mean value of the dominant signal. This result suggests that they are generated by two Nile Red molecules interacting with the same vesicle during the same burst period. This idea was confirmed by increasing the concentration of Nile Red in the solution by ∼15 times to obtain the intensity−time record shown in Figure 4b_1. The count rate distribution, shown in Figure 4b_3, now shows an additional peak centered at ∼110 counts/ms, which is about twice the signals observed for one molecule at 57 counts/ms. At such a high concentration, three molecules having overlapping bursts have also been observed, as shown by the very weak peak around ∼174 counts/ms in Figure 4b_3. One such burst is marked as 3 in Figure 4b_2. At the low concentrations used in all subsequent experiments, shown in Figure 4a_3 there is only a very weak peak near ∼110 counts/ms, indicative of the very small probability of observing simultaneous bursts from two molecules under these conditions. The data we present show that, by confining the target molecules in a volume much smaller than the focused laser beam, we can clearly tell how many target molecules exist in the probe volume from the detected fluorescence intensity. This result may have application in sorting at the single molecule level. For example, by using the method described here, target molecules labeled with one dye, two dyes, or multiple dyes can be distinguished, and their populations can be determined. Another application might arise if dye-labeled molecules form aggregates, because then the different oligomers in the solution could be distinguished by the method.

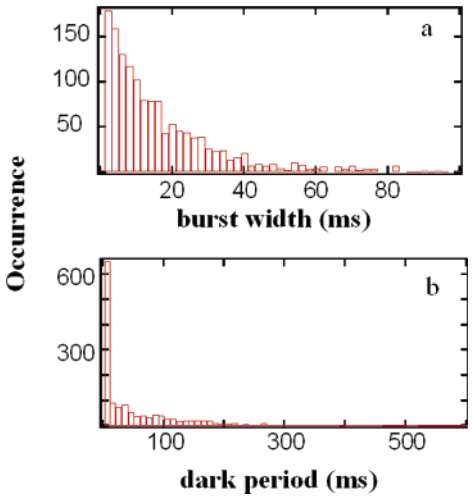

Figure 5. Fluorescence burst width (a) and dark period (b) distributions associated with a single DMPC vesicle on a glass surface. The mean burst width and mean dark period for this particular vesicle were determined to be 16 ms and 162 ms, respectively.

The frequency of observed fluorescence bursts in the experiment is determined by the concentration of Nile Red in solution, as illustrated in Figure 4a_1 and Figure 4b_1, the diffusion coefficient of Nile Red, and the size of the vesicle (see the discussion below). To determine the widths of the fluorescence bursts and associated dark periods in the intensity−time records, the following data analysis procedure is used. Each intensity−time record was first filtered by single pass binominal smoothing (Igor Pro, Wavemetrics), and then a threshold was carefully selected to calculate the fluorescence burst widths and the lengths of the dark periods, as shown in Figures 3, 4a_2 and 4b_2. The burst width is the time interval during which the continuous fluorescence signal is above the threshold. The dark period is the time interval during which the signal is below threshold. As an example, Figure 5 shows the histograms of fluorescence burst widths and dark periods associated with a typical single DMPC vesicle adsorbed on glass. The mean fluorescence burst widths and mean dark periods associated with each vesicle are then used to generate the distribution of mean on-times and distribution of mean off-times averaging over many vesicles, as shown in Figure 6. There was no measurable correlation from single vesicle experiments either between on-times and the following off-times or between two successive on-times and/or off-times. The same result prevailed after averaging over different vesicles. Accordingly, all the information about the kinetic scheme relating the Nile Red and vesicle is contained in the separate on- and off-time distribution functions, from which the intensity−time records could be reconstructed.[25] The on-time distributions for the individual vesicles were exponential decays. The total fluorescence burst width histograms, obtained by summing the fluorescence burst width histograms from 162 single DMPC/SOPC vesicles, also fitted well to a single exponential decay, as shown in Figure 7 which clearly demonstrates that Nile Red resides for longer mean times in DMPC than in SOPC. In contrast, the total histograms of the dark periods associated with all the single DMPC and SOPC vesicles are similar to each other and distinctly not single exponential. In Figure 7 the dark period data are fitted to a double exponential decay having components at ∼1 ms and ∼150 ms.

(33) Chen, Y.; Muller, J. D.; So, P. T. C.; Gratton, E. *Biophys. J.* **1999**, *77*, 553−567.

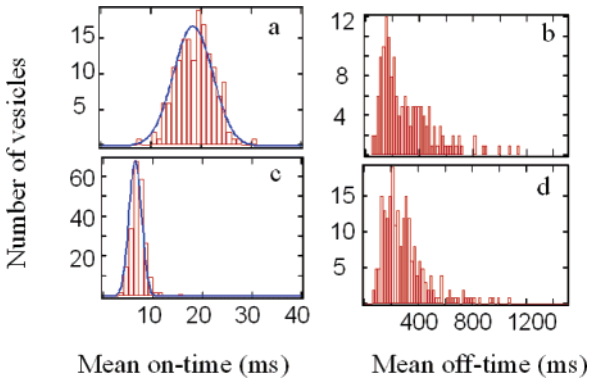

Figure 6. Vesicle dependence of the mean on- and off-times for DMPC (a and b) and SOPC (c and d). By fitting to Gaussians, the mean on-time for DMPC vesicles is determined to be 18.3 ms with a standard deviation of 5.8 ms. For SOPC, the mean and standard deviation are 6.4 ms and 1.7 ms.

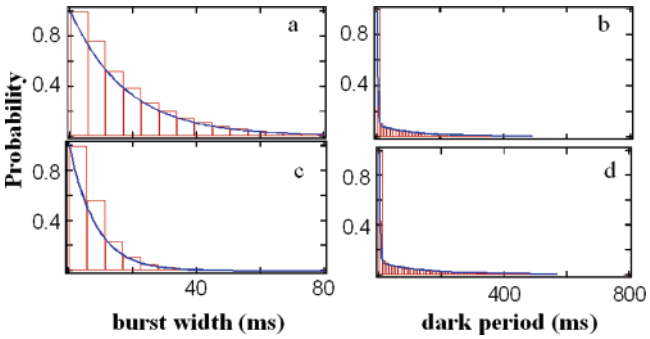

Figure 7. Probability distributions of the widths of fluorescence bursts from all the immobilized single DMPC (a) and SOPC (c) vesicles and of the dark periods associated with all the single DMPC (b) and SOPC (d) vesicles. The solid lines in the graphs are single exponential or double exponential fits to the data, which involved averaging over ~200 vesicles.

For comparison, tetramethylrhodamine (TMR) or rhodamine 6G (Rh6G) molecules were also examined in the presence of ~1 pM DMPC vesicles isolated on glass surfaces, and the images were recorded in the same manner as that for the Nile Red experiments. For both rhodamine probes a spatially homogeneous fluorescence background developed as the concentration was increased. This is expected if the dyes are not binding to any region of the surface, lipid or glass, for sufficient time to be identified as bright single molecule signals. When Nile Red (~0.3 nM) was added to this solution, similar bright fluorescence spots to those in Figure 2 were recovered, but with reduced signal-to-noise ratio because of the increased background generated by existing rhodamine dyes in solution. Because TMR and Rh6G have sizes and diffusion coefficients that are similar to those of Nile Red, perhaps it is their positive charge combined with their greater polarity compared with those of the hydrophobic Nile Red that diminishes their association with lipids.

Discussion

The detailed theory of the results reported here, which will be the subject of a future publication, requires a full treatment of a diffusion controlled reaction including geminate effects. A quantitatively based descriptive picture of the processes being measured will be given here. The observables in the experiment are the on- and off-time probability distributions P_{on} and P_{off} of the fluorescence signals. For example the mean off-time, τ_{off}, is obtained from $\langle\tau_{off}\rangle = \sum\tau_{off}P_{off}(\tau_{off})$, where $P_{off}(\tau)$ is the off-time probability histogram. A Nile Red molecule must diffuse from the bulk to the vesicle and make contact with it. The intervals between such collisions must be controlled by the inverse of the rate of a diffusion controlled reaction. On collision with the vesicle the probe may still be in contact with water and so it may or may not be fluorescent: we refer to this configuration as a contact pair, analogous to experiments on fluorescence quenching. The probe may then interact with the vesicle more substantially or even require penetrating into it: this action certainly gives rise to a Nile Red fluorescence burst. After a few milliseconds, that particular probe molecule will return to being a contact pair and then may either diffuse into the bulk or react again with the vesicle producing another fluorescence burst: following the release of the probe from the vesicle there must arise a nonequilibrium distribution of probes in the solution. Clearly there are at least three time scales involved in the experimental signals: one is dominated by the time of diffusion of bulk molecules to the vesicle which in the present experiments is ca. 200 ms, the mean off-time averaged over many vesicles; another, ca. 1 ms process is due to a reversible fluorescence quenching that occurs when the Nile Red and vesicle are in close contact; and the third is connected with the overall lifetime of a fluorescent Nile Red−vesicle pair, corresponding to the mean on-time of the fluorescence which is in the range 5−20 ms. These stages are illustrated in Figure 3, which is an expanded scale version of the typical experiments shown in Figure 4. The interval τ_1 is clearly a separation between bursts and is the time during which bulk diffusion is occurring. The time τ_2 is the effective length of a burst which relates to the time that a particular Nile Red molecule remains in close contact with the vesicle. At the lowest concentrations used in the experiments, the intervals between bursts are sufficiently long that the probability of detecting two overlapping bursts is completely negligible. However, the short component of the τ_{off} distribution is still significant when $\langle\tau_{off}\rangle$ = 700 ms. The intervals τ_3 correspond to intermittent fluorescence quenching during the lifetime of a particular pair which can include the probe revisiting the vesicle from the contact pair and perhaps photophysical and/or photochemical processes. Therefore we expect that the off-time distribution as we have defined it operationally will involve the two time scales τ_1 and τ_3. In a particular trajectory there occur some off-times that are long compared with the mean value. These regimes correspond to the system approaching complete dissociation of the complex. The complete relaxation kinetics of the proposed scheme is contained in the autocorrelation function of the trajectories, so we have investigated whether these deviations approach zero according to a power law.[27]

Lipid Dependence of On-Time Distributions and Heterogeneity. The lipids, DMPC and SOPC have different gel-fluid phase transition temperatures, ~24 °C and 6 °C, respectively. At the experimental temperature of 25 °C, SOPC should be almost entirely in the fluid phase. The phase behavior of supported DMPC bilayers on Mica[34−37] and on microscope

(34) Feng, Z. V.; Spurlin, T. A.; Gewirth, A. A. *Biophys. J.* **2005**, *88*, 2154−2164.
(35) Enders, O.; Ngezahayo, A.; Wiechmann, M.; Leisten, F.; Kolb, H. A. *Biophys. J.* **2004**, *87*, 2522−2531.
(36) Charrier, A.; Thibaudau, F. *Biophys. J.* **2005**, *89*, 1094−1101.

coverslips[38] has been widely studied by atomic force microscopy (AFM)[34−37] and by fluorescent recovery after photobleaching (FRAP).[38] Both AFM and FRAP indicated that for supported DMPC bilayers the gel phase coexists with the fluid phase even when the temperature is at ∼5 °C above the gel-fluid phase transition temperature of ∼24 °C. The published results clearly indicate that DMPC vesicles should adopt a complex multiphase structure under our experimental conditions.

Our experiments were done in the same manner for both DMPC and SOPC vesicles, including the experimental setup, excitation power, data collection and data analysis, temperature, glass coverslips, vesicle preparation, Nile Red concentration, and so on. However, the measured mean residence time of Nile Red in DMPC is about 3 times longer than that in SOPC, as shown in Figures 6 and 7. As discussed above, at 25 °C SOPC is mainly in the liquid crystalline phase and has considerable mobility. In contrast, DMPC lipids are near the phase transition where the ordered gel and disordered liquid crystalline phase coexist.[34−38] Therefore, the Nile Red residence time in DMPC vesicles might be longer than that in SOPC vesicles because the gel phase traps the probe more effectively. This expectation is consistent with the experimental results shown in Figures 6 and 7 and with the discussion of equilibrium constants given later. The on-time distributions in Figure 6a and 6c represent the heterogeneity of the mean residence times of Nile Red. Comparisons of Figure 6a and 6c show that the distribution widths are very different for the two lipids. It is broader for DMPC indicating more structural heterogeneity compared with SOPC. The mean of the size distributions for DMPC and SOPC vesicles appear to be similar to each other according to the data discussed below (Figure 9), but the variance in size is considerably larger for DMPC. According to Figure 1 there are no obvious differences in the fluorescence spectra seen in the two lipids.

Previous work has shown that LUVs flatten considerably upon adsorption to glass surfaces[5,39] and that they stay on glass as intact vesicles, partially broken vesicles, and lipid bilayer disks. Our experiments, based on the detection of the fluorescence of single Nile Red molecules bound to the lipid bilayers, cannot directly establish structure differences among these membranes because the vesicle−Nile Red interaction is not yet fully understood. The results given in Figure 6a and 6c need to be evaluated in terms of vesicle size and shape, lipid mobility variations, possible heterogeneity caused by vesicle preparation, and so on. The observed heterogeneity for both DMPC and SOPC vesicles is certainly influenced by the glass surface. The DMPC vesicles at 25 °C being closer to the phase transition are possibly more readily affected by the surface than those of SOPC.

It can be expected that the fluorescence burst width distribution from a single vesicle would provide information on the inherent microscopic heterogeneity associated with the vesicle. The majority of the fluorescence burst width distributions associated with immobilized single DMPC or SOPC vesicles, as shown in Figure 5a, exhibit a single-exponential decay as

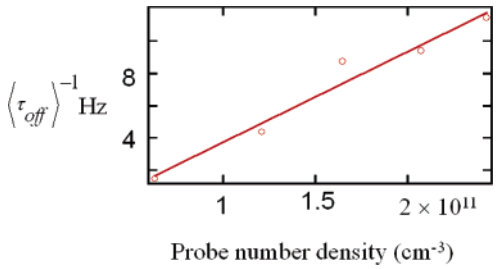

Figure 8. Inverse mean off-times, $\langle \tau_{off} \rangle^{-1}$, vs Nile Red concentration for a typical DMPC vesicle on a glass surface. The straight line is a least-squares fit to a linear relation.

do the total histograms of the fluorescence bursts shown in Figure 7a and 7c.The diffusion coefficient of dye-labeled lipid molecules diffusing on the DMPC monolayer has been measured by several groups[40,41] to be $\sim 2 \times 10^{-8}$ cm^2 s^{-1}. If this value is used as a lower limit for the lateral diffusion coefficient of Nile Red diffusing in DMPC, the time for a Nile Red molecule to traverse a 100 nm vesicle is estimated to be less than 310 μs. During the residence times of 6−18 ms, a Nile Red molecule could traverse the 100 nm vesicle at least 20 times on average, which should certainly allow it time to probe both phases of DMPC during each individual visit. A few vesicles exhibited fluorescence burst width distributions that could not be fitted by a single exponential decay. Two or more well-distinguished microdomains associated with different phases could be the reason. The time scale of the dynamic exchange between the microdomains must be slower than the Nile Red/vesicle association time, 18 ms for DMPC and 6 ms for SOPC. When more fully understood these properties will allow Nile Red to be used as a probe to study the heterogeneity and structural fluctuations of more complex membrane structures, such as mixed bilayers of various lipids or cell membranes.

Off-Time Distributions and Vesicle Size Distributions. Figure 7 shows that the dark periods in the intensity−time records associated with both DMPC and SOPC vesicles have two characteristic time scales, one of ∼1 ms and another of ∼150 ms, with the latter corresponding closely to the expectations for the conventional diffusion-controlled collision rate. The ∼1 ms dark period may correspond to a situation where one Nile Red molecule partially dissociates and then revisits the vesicle surface, but it could also involve some Nile Red photophysics and/or photochemistry. In separate experiments, the ∼1 ms component was measured to be independent of Nile Red concentration over the range displayed in Figure 8. Moreover, when the dark periods exceed 700 ms on average, which occurs in the most dilute solutions, the 1 ms dark period is still observed. Clearly this transient does not correspond to a bulk diffusion controlled reaction. One hypothesis is that while trapped or very close to the vesicle, Nile Red molecules can be exposed to water intermittently (∼1 ms time scale) resulting in intermittent quenching of the fluorescence.

The theory of diffusion controlled reactions[26] indicates that the collision frequency of a particle that is small compared with a hemispherical object of radius R lying flat on a surface is given by $\tau_R^{-1} = 2\pi RDN$, where D is the particle translational diffusion coefficient in the solution and N is the number of particle number density per cm^3. Several groups have found

(37) Tokumasu, F.; Jin, A. J.; Feigenson, G. W.; Dvorak, J. A. *Ultramicroscopy* **2003**, *97*, 217−227.
(38) Jin, A. J.; Edidin, M.; Nossal, R.; Gershfeld, N. L. *Biochemistry* **1999**, *38*, 13275−13278.
(39) Schönherr, H.; Johnson, J. M.; Lenz, P.; Frank, C. W.; Boxer, S. G. *Langmuir* **2004**, *20*, 11600−11606.
(40) Forstner, M. B.; Kaes, J.; Martin, D. *Langmuir* **2001**, *17*, 567−570.
(41) Ke, P. C.; Naumann, C. A. *Langmuir* **2001**, *17*, 3727−3733.

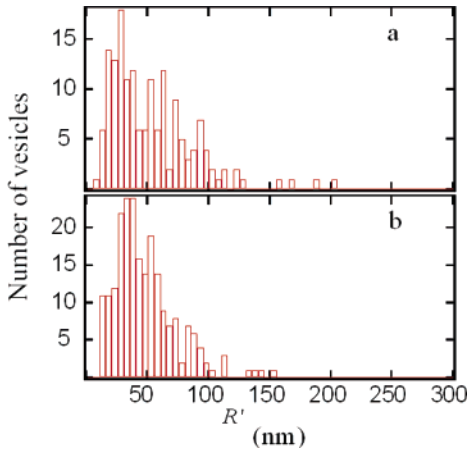

Figure 9. Vesicle size parameter, R', distributions as defined in the text calculated from the $\langle\tau_{off}\rangle^{-1}$ of individual intensity−time records. (a) DMPC, (b) SOPC.

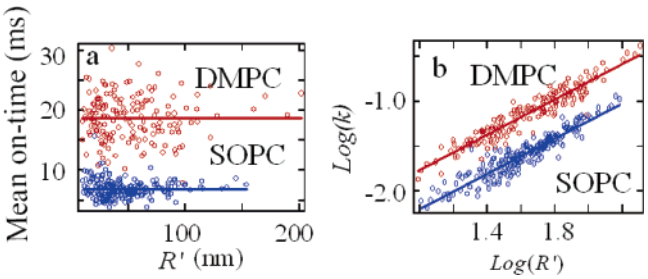

Figure 10. (a) Variation of the mean on-time with radius R' (obtained as described in the text) of individual vesicles. (b) Log(k) (defined in the text) versus log(R'). The solid lines have slopes of unity. Each of the points in (a) and (b) represent an individual vesicle.

that the ca. 100 nm vesicles on glass surfaces have shapes resembling hemispheres.[39,42] The obvious interpretation of the dark periods between the fluorescence bursts is that they represent the intervals between collisions of freely diffusing Nile Red molecules with the immobilized vesicles. The mean dark period $\langle\tau_{off}\rangle$ obtained from the fluorescence intensity−time record on a single vesicle is then expected to be inversely proportional to the Nile Red concentration in solution, the vesicle size, and the bulk translational diffusion coefficient of Nile Red in solution. Accordingly, $\langle\tau_{off}\rangle^{-1} = \alpha\beta/\tau_R$ where α is the probability that a collision will result in a fluorescence burst and β is a shape factor discussed later. A linear relationship was found between $\langle\tau_{off}\rangle^{-1}$ and the concentration of Nile Red, as shown in Figure 8 for one typical vesicle. The linearity indicates that the measured values of $\langle\tau_{off}\rangle^{-1}$ are proportional to the sizes of the vesicles. To obtain a vesicle size, it is necessary to know the value of D in water where Nile Red does not fluoresce significantly. From the value of $D = 1.9 \times 10^{-6}$ cm^2 s^{-1} in chloroform,[17] we obtained the value in water by means of the Stokes Einstein relation, which yields: $D = 1.1 \times 10^{-6}$ cm^2 s^{-1}. The off-time measurements on large numbers of vesicles were then processed for sizes according to the relationship: $R' = \alpha\beta R(\text{nm}) = 1.45 \times 10^{12}\langle\tau_{off}\rangle^{-1}/N$. For the typical vesicle shown in Figure 8 and assuming $\beta = 1$, corresponding to a hemisphere (for a flat circular disc,[43] $\beta = 2/\pi$), and $\alpha = 1$, the value of R is found to be 81 nm.

The distribution of the sizes R' of individual vesicles is shown in Figure 9. The actual shapes of the immobilized vesicles on glass are unknown, and it can be expected that they are not perfectly symmetric, so that the vesicle radius R' as measured by our experiments is regarded as a mean size parameter of the vesicle. However the difference between a circular,[43] a hemispherical, and even cylindrical object[44] is small, and hence the corrections to the size parameter from the shape dependence are also expected to be relatively small within a reasonable range of shapes. The distributions clearly indicate the heterogeneity in the sizes of vesicles adsorbed on glass. From Figure 9a and 9b, it is clear that for both DMPC and SOPC vesicles the R' distributions are broad and in the range 10−100 nm. Neither of these two distributions fitted well to a Gaussian. However the mean radius of ∼50 nm is consistent with the vesicle preparation procedure in which both DMPC and SOPC vesicles were extruded through polycarbonate membranes having a 100 nm pore diameter. The obtained radius distributions are also in good agreement with the AFM experimental results reported for similarly prepared vesicles.[39,42] Some of the factors currently beyond our control that might affect the accuracy of the radius distributions are the following: the value of α for individual vesicles (see below); small errors in the Nile Red concentration; the subjective selection of bright fluorescence spots for the intensity−time records; the sample preparation procedure; and the use of several different glass coverslips or several different regions of the same glass coverslip. Nevertheless, because the experimental results with $\alpha\beta \approx 1$ are consistent with the AFM observations, the expectations from the sample preparation method, and the hard sphere collision theory, the results indicate that the subdiffraction limited size parameters of the vesicles can be directly assessed by the method described here.

Association and Dissociation of Nile Red and Lipids. The residence time of a Nile Red probe freely diffusing in the focus of a laser beam having a width of 500 nm at $1/e^2$ is ∼250 μs.[8] However, the average residence time found for Nile Red on a vesicle with a diameter of 100 nm is 18 ms for DMPC and 6 ms for SOPC. As discussed above, the time for a Nile Red molecule to traverse a 100 nm vesicle is estimated to be less than 310 μs. Therefore the Nile Red molecules must be associated with the lipids in such a way that the observed long residence time is not mainly determined by this translational diffusion process. Furthermore, if Nile Red molecules were undergoing two-dimensional lateral diffusion in the lipid bilayers, the mean on-times would be influenced by the effective diameters of the vesicles.[41] However the results in Figure 10a show that there is no dependence of the mean on-times on the R' values for either DMPC or SOPC vesicles. The repeated association and dissociation of single Nile Red molecules with a vesicle at equilibrium is demonstrated by the fluctuating on-and-off signals in the fluorescence intensity−time records, for example, in Figure 4. The fluorescence bursts in the intensity−time records represent the associated states, and the dark periods represent the dissociated states. The experiments suggest that membrane dynamical fluctuations have a role in the dissociation of Nile Red probes from the lipids, because longer residence times were found for DMPC, which has a gel phase present that is more viscous than the liquid phase.[38]

As described above, the binding and dissociation of Nile Red molecules to an immobilized vesicle as described here should

(42) Reviakine, I.; Brisson, A. *Langmuir* **2000**, *16*, 1806−1815.
(43) Shoup, D.; Lipari, G.; Szabo, A. *Biophys. J.* **1981**, *36*, 697−714.
(44) Chekunaev, N. I. *Chem. Phys.* **2004**, *300*, 253−266.

first be treated as a diffusion-influenced reversible reaction, such as NV $\underset{k_2}{\overset{k_1}{\rightleftharpoons}}$ N···V $\underset{k_4}{\overset{k_3}{\rightleftharpoons}}$ N + V. In that case, V could be the vesicle, and NV is fluorescent Nile Red associated with the vesicle. The contact or geminate pair N···V is in exchange with NV and N + V and it is nonfluorescent: its presence in the scheme permits the revisiting of N with V to creat NV on short time scales. Figure 3 shows an expanded view of the bursts in a very dilute solution where $\langle\tau_{off}\rangle = 700$ ms. During a burst the fluorescence is mainly above threshold and only infrequently undergoes quenching. If the burst dynamics corresponds mainly to the NV $\underset{k_2}{\overset{k_1}{\rightleftharpoons}}$ N···V interchanges, the on-time, $1/k_1$, is much longer than the short off-time component $1/k_2$, but both k_2 and k_1 are significantly larger than the diffusion controlled rate k_4N; in other words, at the low concentrations the mean on-time of ca. 5−30 ms is much less than the diffusion controlled mean off-times that were observed and summarized in Figure 6. With this analysis the slow component is mainly diffusion controlled association of Nile Red with the vesicle (k_4) and the $\langle\tau_{on}\rangle$ represents the mean burst width $\langle 1/k_1\rangle$. This picture predicts that the off-time distribution will contain a fast component that generates off-states only during the bursts corresponding to the system being in the geminate pair state. $P_{on}(t)$ is a single exponential decay with a time constant of k_1 corresponding to the fluorescence quenching. Because $\langle\tau_{on}\rangle$ is independent of R' (Figure 10a), the factor of $\langle\tau_{on}\rangle/\langle\tau_{off}\rangle = k$ is expected to be linearly dependent on R'. Indeed the plot of log(k) versus log(R') shown in Figure 10b accurately exhibits a slope of unity. Figure 10b also shows that Nile Red binds to DMPC more strongly than to SOPC vesicles. The mean values of k/N for the reactions of Nile Red with DMPC and SOPC vesicles, as defined above, are determined to be 4.5×10^8 M^{-1} and 1.5×10^8 M^{-1}. These are within a factor of order of the equilibrium constants.

The long time part of the off-time probability density distribution dominantly behaves as the half reaction exp[$-k_4'Nt$], where k_4' is close to the Smoluchowski diffusion controlled rate constant k_4 times a factor of order unity. It is therefore interesting to examine this distribution for values of the off-time that greatly exceed $\langle\tau_{off}\rangle$. For a reversible bimolecular reaction like the one described here, it is predicted theoretically[28,45] that the concentrations relax to their equilibrium values as $ct^{-3/2}$, where the constant c is determined by the equilibrium constant of the reaction, the diffusion coefficient, and the equilibrium concentrations. We examined the off-time distribution calculated from individual single intensity−time records to discover if they exhibit power law behavior at long off-time scales where $\tau_{off} \gg \langle\tau_{off}\rangle$. Clearly the signal begins to deviate from exponential at long times, but there is a large noise contribution at the individual vesicle level. The data in Figure 11 are an average over many trajectories taken from a narrow distribution of sizes as extracted from Figure 9b and shown in the inset of Figure 11. The data in Figure 11 show off-times up to 5 or 6 times the mean value where the probability has dropped to ca. 0.004. However there is no evidence for power law behavior in this experiment. It should be noted that for off-times around 1 s the diffusion distance scale being probed, $\sqrt{Dt} \approx 10$ μm, is approaching the sample dimensions and is certainly much larger than the separation between the vesicles on the surface of 1−2 μm (see Figure 2). Effects arising from the very large scale of the diffusion at large off-times will require being understood in order to interpret the long time scale shape of the distribution in Figure 11.

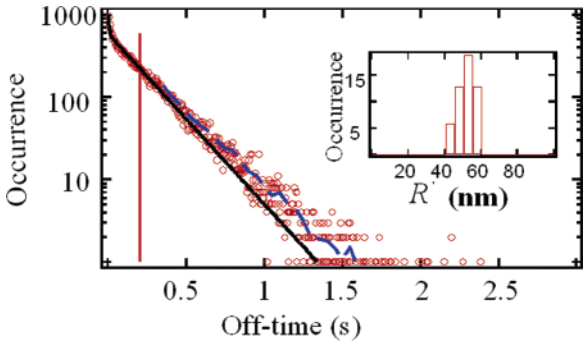

Figure 11. Sum of the off-time distributions (circles represent 5 ms wide histogram amplitudes) calculated from 51 individual intensity−time records. The solid vertical line draws attention to the mean of the off-times. The dashed curve through the data (>300 ms) corresponds to a 10 point smoothed curve (equivalent to 50 ms smoothing). The solid curve through the data represents a double exponential fit with time constants of ~1 ms and ~209 ms. The inset shows the size distribution of those 51 vesicles.

The individual bursts exhibit intermittent fluorescence behavior where, during the burst and while a single probe is interacting with the vesicle, there are sudden drops in fluorescence signal followed by recovery. These fluctuations show up in the off-time distribution analysis as the fast ~1 ms component in Figure 7b and 7d. The blinking behavior is thought to be from Nile Red molecules in a loosely associated complex with the lipid vesicle surface. The vesicle structure fluctuations may then periodically expose the adsorbate to solvent, quenching its fluorescence while it is still associated with the surface. There are other common causes of intermittency in single molecule fluorescence signals: one is the intervention of triplet states, but the off-times of ~1 ms appear to be too long for triplet lifetimes in solution in the presence of oxygen;[46,47] another is rotational motion, which would be expected to be too fast[48] to cause the observed millisecond drops in fluorescence. The data reported here do not provide a measurement of α, the fraction of collisions that leads to a measurable fluorescence burst. However, the self-consistency of the data analysis, including calculation of the collision frequency and the shapes of the off-time distributions, suggests that α is in the range of unity. Future experiments will attempt to measure α directly and to define more clearly how Nile Red is incorporated into the lipid bilayer.

The normalized time autocorrelation functions of the trajectories (such as those in Figure 3) were biexponential with the longer time constant being approximately given by the on-time and the shorter one being the sum of all four rates in the scheme. This type of biexponential relaxation kinetics is indeed the expectation for the deviations of any of the concentrations in the foregoing geminate model from their equilibrium values.[49] The autocorrelation function in Figure 12 was obtained by averaging autocorrelations of the various trajectories from vesicles chosen to have very similar sizes. Besides displaying the biexponential relaxation kinetics, the averaged correlation

(45) Gopich, I. V.; Doktorov, A. B. *J. Chem. Phys.* **1996**, *105*, 2320−2332.
(46) Mei, E.; Vinogradov, S.; Hochstrasser, R. M. *J. Am. Chem. Soc.* **2003**, *125*, 13198−13204.
(47) Yip, W.-T.; Hu, D.; Yu, J.; Vanden Bout, D. A.; Barbara, P. F. *J. Phys. Chem. A* **1998**, *102*, 7564−7575.
(48) Das, T. K. *J. Phys. Chem.* **1996**, *100*, 20143−20147.
(49) Laidler, K. J. *Chemical Kinetics*, 2nd ed.; McGraw-Hill: New York, 1965.

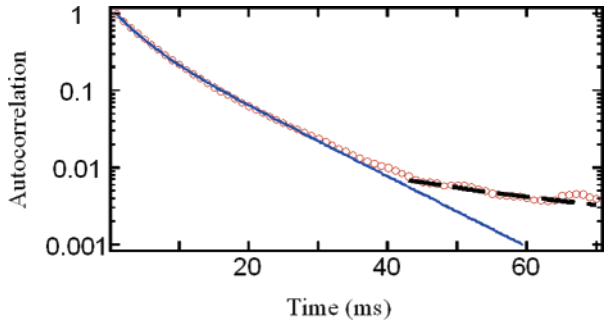

Figure 12. Average autocorrelation function (○) of the complete on/off trajectory calculated by using the same 51 intensity−time records as used in Figure 11. The solid curve through the data represents a double exponential fit to the data with time constants of 3.3 ms and 9.5 ms. The dashed line overlapping with the tail of the data represents the fit using a power law of $t^{-3/2}$. The statistical mean of on-times for the 51 trajectories is measured to be 5.6 ms, and the off-time probability density distribution is given in Figure 11.

function appears to deviate from exponential at long times, exhibiting a region resembling power law behavior. The averaging over many vesicles required for the autocorrelation function in Figure 12 is not the ideal approach for this experiment, and therefore future work will report on both experiments and theory for trajectories from single vesicles that are optimized to test the theoretical predictions.

Conclusions

The interaction of Nile Red molecules with ∼100 nm phospholipid vesicles adhered to glass has been studied by single molecule fluorescence confocal spectroscopy. The collisional frequency and residence times of Nile Red in vesicles were directly measured from the fluorescence intensity−time records. The method is free from photobleaching so that trajectories can be examined for very long time periods. The experimental results showed that different bilayers, whose lipid molecules have different mobility, different interaction forces, and different fluctuation dynamics, are differentiated on the basis of the exponentially distributed residence times of Nile Red in the vesicles. Although the average diameter of vesicles (∼100 nm) is much less than the $1/e^2$ diameter of the focused laser beam (500−600 nm), the experiments based on measurements of the off-time distributions demonstrate that sizes of nanomembrane structures that are much smaller than the optical diffraction limit of the confocal microscope can be estimated. The equilibrium constant of the Nile Red−vesicle reaction have been obtained based on the measured association and dissociation rate constants of the reaction. The vesicle and environment sensitive probe described here is a useful model with which to study reversible diffusion controlled bimolecular reactions.

The experiments show that Nile Red is a useful probe with which to image hydrophobic regions within a surrounding aqueous medium, and therefore it has potential in studies of protein conformational fluctuations. Nile Red is also shown to be a feasible single molecule probe for studying the heterogeneity and structural fluctuations of complex membrane structures, such as mixed bilayers of various lipids, and may be useful for cell membranes. Furthermore, because the vesicles are immobilized on glass, they could prove useful in confining single membrane proteins[50] in hydrophobic environments, analogous to the recent experiments with tethered reverse micelles.[10]

Acknowledgment. This work was supported by NIH Grants GM48130 and RFA-RM-04-001 using instrumentation developed by the NIH Research Resource Grant NIH P41RR001348.

JA058098A

(50) DeGrado William, F.; Gratkowski, H.; Lear James, D. *Protein Science* **2003**, *12,* 647−665.